INTERNATIONAL JOURNAL OF FLUID POWER, 2017
VOL. 18, NO. 3, 153–166
https://doi.org/10.1080/14399776.2017.1380348

Taylor & Francis
Taylor & Francis Group

Reduced-order modelling of transient flow in transmission lines using distributed lumped parameters

Taoufik Wassar[a], Matthew A. Franchek[a] and José A. Gutierrez[b]

[a]Department of Mechanical Engineering, University of Houston, Houston, TX, USA; [b]Technology and Innovation Department, Transocean, Houston, TX, USA

ABSTRACT

Developed in this paper are mathematical models capturing the one-dimensional underdamped dynamics of confined fluid flow within cylindrical transmission lines. The resulting models are rational transfer functions with coefficients that are explicit functions of the fluid properties and line geometry. Unlike a traditional lumped-parameter approach, the accuracy of the fluid resonant frequencies predicted by the proposed models is precise and not a function of transmission line axial discretisation. Therefore, model order (complexity) is solely a function of the number of desired modes, which in turn influences pressure and flow predictions. The results are applicable to both laminar and turbulent flow. To develop the models, a distributed lumped-parameter approach is employed. Specifically, a quasi-steady state friction approximation is used within the governing partial differential equations. The solution to the linearised ordinary differential equations produces three transcendent transfer functions that are approximated using finite-order rational transfer functions. The parameters of resulting transfer functions are then modified to capture the second-order effects. A fluid power design example using the proposed model is provided to illustrate the utility of these models.

ARTICLE HISTORY
Received 18 August 2016
Accepted 9 March 2017

KEYWORDS
Transmission line dynamics; distributed lumped parameters; second-order effects; fluid power system design

1. Introduction

Transient fluid flow in a transmission line is governed by the Navier-Stokes equations (Rufelt 2010). With general closed-form solutions not known, numerical solutions including 'method of characteristics', 'transmission line method', 'Galerkin finite method', and 'finite element methods' have prevailed (Streeler and Lai 1962, Rachford and Ramsey 1975, Rao and Eswaran 1993, Soumelidis *et al.* 2005, Manhartsgruber 2006, Kogler *et al.* 2007, Johnston 2012). These methods are computationally expensive and the resulting solutions do not directly translate into compact models having utility in system design, control design, and system condition and performance monitoring. Advancements have been made to develop reduced-order models that balance prediction accuracy against solution complexities (Manhartsgruber 2005). Iberall (1950) and Gerlach (1969) derived exact first-order solutions that included viscous friction effects from the basic laws of conservation of momentum, conservation of mass and equations of state. Consider the case of non-turbulent mean flow, Mach number much less than unity, a low diameter-to-length ratio, a low normalised density variation and neglecting convective terms. The governing partial differential equations for confined fluid flow under these conditions are

$$\text{Momentum equation:}\quad \bar{\rho}\frac{\partial u}{\partial t} = -\frac{\partial P}{\partial x} + \left(\frac{\partial^2 u}{\partial r^2} + \frac{1}{r}\frac{\partial u}{\partial r}\right), \tag{1}$$

$$\text{Continuity equation:}\quad \frac{\partial \rho}{\partial t} + \bar{\rho}\left(\frac{\partial u}{\partial x} + \frac{\partial v}{\partial r} + \frac{v}{r}\right) = 0, \tag{2}$$

$$\text{Liquid state equation:}\quad \frac{\mathrm{d}\rho}{\mathrm{d}\bar{\rho}} = \frac{\mathrm{d}P}{\beta_e}, \tag{3}$$

$$\text{Gas state equation:}\quad \frac{\mathrm{d}\rho}{\mathrm{d}\bar{\rho}} = \frac{\mathrm{d}P}{\gamma \bar{P}}, \tag{4}$$

where x [m] and r [m] are independent cylindrical space variables, and t is the independent time variable. The dependent fluid variables include pressure P [Pa], its time average $\bar{P}$, velocities in x-direction and r-direction (u and v [m/s]), density ρ [kg/m^3], its time average $\bar{\rho}$, fluid absolute viscosity μ [kg/m/s], fluid effective bulk modulus β_e [Pa] and specific heat ratio γ.

The results found by Iberall (1950) and Gerlach (1969) were extended by Goodson and Leonard (1972)

CONTACT Taoufik Wassar twassar@central.uh.edu

to create 'the dissipative model' that includes the heat transfer effects, which are mainly defined as radial heat transfer effects. In fact, using the energy equation, the axial heat transfer term is negligible when compared with the radial heat transfer terms (Brown 1962). The resulting analytical solution produces a transfer function matrix relating the line pressure and flow rate variables at the inlet ($P_{in}(s)$, $Q_{in}(s)$) and outlet ($P_{out}(s)$, $Q_{out}(s)$). The transfer functions are transcendental functions of the transmission line propagation operator Γ and characteristic impedance Z_c (Goodson and Leonard 1972):

$$\begin{bmatrix} P_{out}(s) \\ Q_{in}(s) \end{bmatrix} = \begin{bmatrix} \cosh^{-1}(\Gamma) & -Z_c \tanh(\Gamma) \\ Z_c^{-1} \tanh(\Gamma) & \cosh^{-1}(\Gamma) \end{bmatrix} \begin{bmatrix} P_{in}(s) \\ Q_{out}(s) \end{bmatrix}. \tag{5}$$

The *dissipative model* of (5) is regarded as an accurate mathematical model for the case of laminar flow (Woods 1981, Stecki and Davis 1986). A limitation of this model is that the transfer functions contain hyperbolic functions that cannot be transformed to the time domain using inverse Laplace Transform methods (Oldenburger and Goodson 1964). To facilitate system analysis and synthesis in the time domain, dissipative modal approximations were developed using infinite product representations of hyperbolic functions (Brown 1962, D'Souza and Oldenburger 1964). The transcendental transfer functions are replaced by finite-order rational polynomial transfer functions, namely:

$$\begin{bmatrix} P_{out}(s) \\ Q_{in}(s) \end{bmatrix} = \begin{bmatrix} \sum_{i=1}^{m} \frac{a_i s + b_i}{s^2 + 2\xi_i \omega_{n_i} s + \omega_{n_i}^2} & -\sum_{i=1}^{m} \frac{c_i s + d_i}{s^2 + 2\xi_i \omega_{n_i} s + \omega_{n_i}^2} \\ \sum_{i=1}^{m} \frac{s(e_i s + f_i)}{s^2 + 2\xi_i \omega_{n_i} s + \omega_{n_i}^2} & \sum_{i=1}^{m} \frac{a_i s + b_i}{s^2 + 2\xi_i \omega_{n_i} s + \omega_{n_i}^2} \end{bmatrix} \begin{bmatrix} P_{in}(s) \\ Q_{out}(s) \end{bmatrix}, \tag{6}$$

where m is the desired number of modes, a_i, b_i, c_i, d_i, e_i and f_i are the ith mode numerator coefficients, ω_{n_i} and ξ_i are the natural frequencies and damping ratios of the ith mode, respectively. The approximation of (5) by (6) mismatches the low frequency gain due to the finite number of modes used in (6) to approximate transcendent transfer functions of (5). Therefore, corrections to the steady-state predictions have been introduced. Yang (1983) proposed a solution in which the numerator coefficients of the approximated transfer functions were rescaled to satisfy the steady-state characteristics of the transcendent transfer functions.

Along with the advancements made in (6) are few distinct challenges remain. The coefficients of the rational polynomial transfer functions in (6) are difficult to obtain because the propagation operator and the characteristic impedance contain zero-order and first-order Bessel functions (Meziou *et al.* 2016). These coefficients are determined either by numerical calculations and/or look-up table (Hsue and Hullender 1983, King 2006). Another drawback of the dissipative modal approximation is that the physical properties of the transmission line are no longer connected to the model coefficients. To overcome these limitations, a solution was proposed by Yang and Tobler (1991) to calculate the model coefficients using a linear friction model. The approach combines the frequency-dependent (unsteady) friction and heat transfer effects into the propagation operator and characteristic impedance. The proposed model is obtained as follows:

$$\begin{bmatrix} P_{out}(s) \\ Q_{in}(s) \end{bmatrix} = \begin{bmatrix} \sum_{i=1}^{m} \frac{\frac{2(-1)^{i+1}\lambda_{c_i}}{D_n \alpha_i^2}}{\bar{s}^2 + 8\frac{\beta_i}{\alpha_i}\bar{s} + \frac{\lambda_{c_i}^2}{\alpha_i^2}} & -\sum_{i=1}^{m} \frac{\frac{2Z_0}{D_n}\left(\bar{s} + 8\frac{\beta_i}{\alpha_i}\right)}{\bar{s}^2 + 8\frac{\beta_i}{\alpha_i}\bar{s} + \frac{\lambda_{c_i}^2}{\alpha_i^2}} \\ \sum_{i=1}^{m} \frac{\frac{2}{D_n Z_0 \alpha_i^2}\bar{s}}{\bar{s}^2 + 8\frac{\beta_i}{\alpha_i}\bar{s} + \frac{\lambda_{c_i}^2}{\alpha_i^2}} & \sum_{i=1}^{m} \frac{\frac{2(-1)^{i+1}\lambda_{c_i}}{D_n \alpha_i^2}}{\bar{s}^2 + 8\frac{\beta_i}{\alpha_i}\bar{s} + \frac{\lambda_{c_i}^2}{\alpha_i^2}} \end{bmatrix} \begin{bmatrix} P_{in}(s) \\ Q_{out}(s) \end{bmatrix}, \tag{7}$$

where $\bar{s}$ is the normalised Laplace operator, Z_0 is the impedance constant, D_n is the dissipation number, λ_{c_i} is the dimensional root index for the ith mode, α_i and β_i are the natural frequency modification factor and damping ratio modification factor for the ith mode, respectively (Yang and Tobler 1991). The modification factors α_i and β_i are a function of the root index λ_{c_i} and captured in non-parametric graphs. Another closed form solution is proposed by Mikota (2013) to approximate the *dissipative model* by finite sums of rational fraction expressions. It is important to note that the reduced-order models in (6)–(7) are only valid for the case of laminar flow, not turbulent flow dynamics in transmission lines.

An alternative solution for modelling fluid dynamics in lines is the lumped-parameter approach (Mamis and Koksal 2000), which consists of lumped transmission line elements using a series of equal length lumped fluid resistance R, inertance I, and capacitance C elements of the system tetrahedron of state (Figure 1).

The corresponding model, in transfer function form, is:

$$\begin{bmatrix} P_{out}(s) \\ Q_{in}(s) \end{bmatrix} = \begin{bmatrix} \frac{\frac{1}{IC}}{s^2 + \frac{R}{I}s + \frac{1}{IC}} & -\frac{\frac{1}{C}s + \frac{R}{IC}}{s^2 + \frac{R}{I}s + \frac{1}{IC}} \\ \frac{\frac{1}{I}s}{s^2 + \frac{R}{I}s + \frac{1}{IC}} & \frac{\frac{1}{IC}}{s^2 + \frac{R}{I}s + \frac{1}{IC}} \end{bmatrix} \begin{bmatrix} P_{in}(s) \\ Q_{out}(s) \end{bmatrix}. \tag{8}$$

This classical approach is a further simplification of underlying systems physics with spatially distributed parameters. For short lines, lumped-parameter modelling could be sufficient. The model in (8) is valid whenever $L \ll 2\pi/\omega_{max}$, where L denotes the length of the line [m], ω_{max} [rad/s] is the maximum frequency anticipated in the line dynamic response and c[m/s] is the speed of sound in the fluid. For long transmission lines where higher frequency modes are present, lumped-parameter modelling is not applicable (Doebelin and Swisher 1970). A simplified model using distributed parameters for both laminar and turbulent flow was presented for longer line scenarios by Matko *et al.* (2000, 2001). The

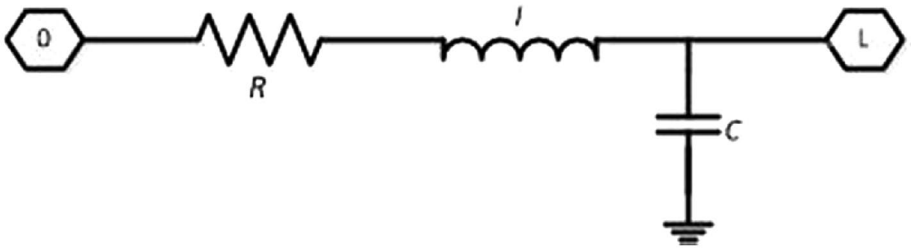

Figure 1. One-element lumped parameter circuit.

resulting models are described in the frequency domain using hyperbolic functions. Three different transcendent transfer functions were developed and then approximated by rational transfer functions using Taylor Series expansion. This work was extended by Blažič *et al.* (2004) to include the changes of the fluid density in the model along with varying pressure and flow rate. The models are compact in that the model parameters contain the physical properties of the fluid and transmission line. However, two major disadvantages of these models are that the resulting models are only valid for the class of well-damped transmission lines, and that unlike the *dissipative model* these models do not take into account second-order effects, namely frequency-dependent friction losses and heat transfer effects.

The focus of this work is the problem of modelling laminar and turbulent flow in transmission lines experiencing pressure and flow oscillations (underdamped lines). The method of solution uses distributed lumped parameters for the fluid dynamics. The resulting models are written in form similar to (6), where the model coefficients are expressed analytically as functions of line and fluid properties and operating conditions. The remainder of the paper is organised as follows. In Section 2, a brief description of the problem and method of solution is provided. In Section 3, the transfer functions presented are approximated by rational polynomial transfer functions, resulting in a model called the '*distributed lumped parameter model*'. By including frequency-dependent (unsteady) friction effects due to viscous losses and heat transfer effects, the model is revised and a new model called the '*modified distributed lumped parameter model*' is developed. A fluid power design example using the proposed model is presented in Section 4 to demonstrate the utility of the proposed model. Concluding remarks are presented in Section 5.

2. Problem statement and method of solution

By neglecting unsteady friction and heat transfer losses, the set of partial differential Equations (1)–(4) describing the dynamics of confined flow in transmission line can be approximated by one-dimensional partial differential equations as:

$$I_x \frac{\partial Q}{\partial t} + R_x Q = -\frac{\partial P}{\partial x}, \tag{9}$$

$$C_x \frac{\partial P}{\partial t} = -\frac{\partial Q}{\partial x}, \tag{10}$$

where the distributed lumped parameters R_x, I_x and C_x are the resistance, inertance and capacitance per unit length (see Appendix 1). It is important to note that, for the case of laminar flow, the resistance per unit length is constant, and therefore, do not depend on the operating conditions. However, for the case of turbulent flow, this resistance depends on the Reynolds number. In this case, the turbulent flow is described as flow superimposed to a turbulent average flow based on the time average of the Reynolds number. Using the Laplace transformation (Matko *et al.* 2001), an analytical solution to (9) and (10) is:

$$\begin{bmatrix} P_{\text{out}}(s) \\ Q_{\text{in}}(s) \end{bmatrix} = \begin{bmatrix} \cosh^{-1}(nL) & -Z_K \tanh(nL) \\ Z_K^{-1} \tanh(nL) & \cosh^{-1}(nL) \end{bmatrix} \begin{bmatrix} P_{\text{in}}(s) \\ Q_{\text{out}}(s) \end{bmatrix}, \tag{11}$$

where

$$n = \sqrt{I_x C_x s^2 + R_x C_x s}, \tag{12}$$

and

$$Z_K = \sqrt{\frac{I_x s + R_x}{C_x s}}. \tag{13}$$

Consider the analytical solution for transient pressure and flow oscillations given in (11). The transfer functions are transcendent (i.e. functions of hyperbolic functions) and do not directly lend themselves to simulations in time domain. The method of solution is to use infinite product series expansion technique to approximate transfer functions in (11) by finite-order rational polynomial transfer functions. This technique is superior to the Taylor series approximation technique used by Matko *et al.* (2000, 2001) because it preserves the poles of the transcendent transfer functions. The resulting model is referred to as the *distributed lumped parameter model* and is written in the form of (6) where the model coefficients are obtained analytically as functions of transmission line geometry, fluid properties and operating conditions for both laminar and turbulent flow cases. Note that two contradictory terms, namely 'distributed'

and 'lumped' are used for the model's name. First, because the transmission line model is obtained using distributed elements, and therefore, the name 'distributed' is used. Second, because these infinite elements are described locally using lumped components notation (resistance, inertance and capacitance per unit length), and therefore, the name 'lumped' is used.

Because the analytical solution of (9) and (10) is derived by assuming that unsteady friction and heat transfer effects are neglected, two frequency-dependent modification factors are included in the *distributed lumped parameter model* to account for these second-order effects (Yang and Tobler 1991). This resulting model is the so-called *modified distributed lumped parameter model*. The modification factors are derived by comparing the natural frequencies and damping ratios of the *distributed lumped parameter model* with those obtained numerically from the approximated *dissipative model*, which is considered as the exact model in the case of laminar flow. Empirical equations are proposed to express these two factors as functions of fluid properties and line geometry.

3. Main results

In this section, the *distributed lumped parameter model* that describes oscillating fluid flow in a transmission line is first developed. Then, this model is adjusted to account for second-order effects, namely frequency-dependent friction losses and heat transfer effects, and the resulting model to develop the *modified distributed lumped parameter model*. The accuracy of this model is finally investigated by comparing its frequency response functions (FRFs) with those of the *dissipative model* presented by King (2006) for the case of laminar flow and with those of the numerical model developed by Johnston (2011a, 2011b) for case of turbulent flow.

3.1. Distributed lumped parameter model

To determine the rational transfer functions, the denominator coefficients are derived by calculating the poles of the three transfer functions in (11). The numerator coefficients can then be obtained by calculating the corresponding residue of each pole. Note that the three transcendent transfer functions in (11) all have the same poles, which are the roots of $\cosh(nL)$ calculated by solving:

$$\cosh(nL) = \prod_{i=1}^{\infty}\left(1 + \frac{n^2L^2}{\pi^2(i-0.5)^2}\right) = 0. \quad (14)$$

In the case of underdamped transmission lines, two complex conjugate poles exist for each second-order mode and are the roots of the following set of equations:

$$I_xC_xs^2 + R_xC_xs + \frac{\pi^2(i-0.5)^2}{L^2} = 0, \forall\, i \le m \quad (15)$$

Provided

$$\frac{L}{\pi}R_x\sqrt{\frac{C_x}{I_x}} < 1. \quad (16)$$

Hence, the corresponding complex conjugate poles of each mode are:

$$\bar{s}_{i,1} = \frac{-R_xC_x + j\sqrt{4\pi^2(i-0.5)^2\,\frac{I_xC_x}{L^2} - R_x^2C_x^2}}{2I_xC_x}, \quad (17)$$

$$\bar{s}_{i,2} = \frac{-R_xC_x - j\sqrt{4\pi^2(i-0.5)^2\,\frac{I_xC_x}{L^2} - R_x^2C_x^2}}{2I_xC_x}. \quad (18)$$

From (17) and (18), the damping ratios and natural frequencies in (6) are:

$$\omega_{n_i} = \frac{\pi(i-0.5)}{L}\frac{1}{\sqrt{I_xC_x}}, \quad (19)$$

and

$$\xi_i = \frac{L}{2\pi(i-0.5)}R_x\sqrt{\frac{C_x}{I_x}}. \quad (20)$$

The numerator coefficients are the corresponding residues calculated using the L'Hôpital's rule (Howie 2004), namely:

$$\begin{aligned}\text{Residue}\left[\cosh^{-1}(nL)\right]_{s=\bar{s}_{i,k}} &= \left[\frac{1}{n'L\sinh(nL)}\right]_{s=\bar{s}_{i,k}} \\ &= \left[\frac{2\pi(-1)^{i+1}(i-0.5)}{(2I_xC_xs + R_xC_x)L^2}\right]_{s=\bar{s}_{i,k}},\end{aligned} \quad (21)$$

$$\text{Residue}\left[Z_K\tanh(nL)\right]_{s=\bar{s}_{i,k}} = \left[\frac{Z_K}{n'L}\right]_{s=\bar{s}_{i,k}}$$

$$= \left[\frac{2(I_xs + R_x)}{(2I_xC_xs + R_xC_x)L}\right]_{s=\bar{s}_{i,k}}, \quad (22)$$

$$\text{Residue}\left[Z_K^{-1}\tanh(nL)\right]_{s=\bar{s}_{i,k}} = \left[\frac{Z_K^{-1}}{n'L}\right]_{s=\bar{s}_{i,k}}$$

$$= \left[\frac{2C_xs}{(2I_xC_xs + R_xC_x)L}\right]_{s=\bar{s}_{i,k}}, \quad (23)$$

where $k = 1, 2$. The numerator coefficients of (6) are:

$$\begin{aligned}a_i = {} & \text{Residue}\left[\cosh^{-1}(nL)\right]_{s=\bar{s}_{i,1}} \\ & + \text{Residue}\left[\cosh^{-1}(nL)\right]_{s=\bar{s}_{i,2}},\end{aligned} \quad (24)$$

$$b_i = -\Big(\bar{s}_{i,2}\text{Residue}\big[\cosh^{-1}(nL)\big]_{s=\bar{s}_{i,1}} + \bar{s}_{i,1}\text{Residue}\big[\cosh^{-1}(nL)\big]_{s=\bar{s}_{i,2}}\Big), \quad (25)$$

$$c_i = \text{Residue}\big[Z_K\tanh(nL)\big]_{s=\bar{s}_{i,1}} + \text{Residue}\big[Z_K\tanh(nL)\big]_{s=\bar{s}_{i,2}}, \quad (26)$$

$$d_i = -\Big(\bar{s}_{i,2}\text{Residue}\big[Z_K\tanh(nL)\big]_{s=\bar{s}_{i,1}} + \bar{s}_{i,1}\text{Residue}\big[Z_K\tanh(nL)\big]_{s=\bar{s}_{i,2}}\Big), \quad (27)$$

$$e_i = \bar{s}_{i,1}^{-1}\text{Residue}\big[Z_K^{-1}\tanh(nL)\big]_{s=\bar{s}_{i,1}} + \bar{s}_{i,1}^{-1}\text{Residue}\big[Z_K^{-1}\tanh(nL)\big]_{s=\bar{s}_{i,2}}, \quad (28)$$

$$f_i = -\bar{s}_{i,1}^{-1}\bar{s}_{i,2}\text{Residue}\big[Z_K^{-1}\tanh(nL)\big]_{s=\bar{s}_{i,1}} - \bar{s}_{i,2}^{-1}\bar{s}_{i,1}\text{Residue}\big[Z_K^{-1}\tanh(nL)\big]_{s=\bar{s}_{i,2}}. \quad (29)$$

Substituting the corresponding poles of each mode defined in (17) and (18) into (21)–(23) and then into (24)–(29) results in:

$$a_i = 0, \quad (30)$$

$$b_i = \frac{(-1)^i(1-2i)\pi}{I_xC_xL^2}, \quad (31)$$

$$c_i = \frac{2}{C_xL}, \quad (32)$$

$$d_i = \frac{R_x}{I_xC_xL}, \quad (33)$$

$$e_i = 0, \quad (34)$$

and

$$f_i = \frac{2}{I_xL}. \quad (35)$$

The resulting approximated model for oscillating pressure and flow rate in a transmission line can be expressed as follows:

$$\begin{bmatrix} P_{\text{out}}(s) \\ Q_{\text{in}}(s) \end{bmatrix} = \begin{bmatrix} \sum_{i=1}^{m} \frac{\frac{(-1)^i(1-2i)\pi}{L^2I_xC_x}}{s^2+\frac{R_x}{I_x}s+\frac{\pi^2(i-0.5)^2}{L^2I_xC_x}} & -\sum_{i=1}^{m} \frac{\frac{2}{LC_x}s+\frac{R_x}{LI_xC_x}}{s^2+\frac{R_x}{I_x}s+\frac{\pi^2(i-0.5)^2}{L^2I_xC_x}} \\ \sum_{i=1}^{m} \frac{\frac{2}{LI_x}s}{s^2+\frac{R_x}{I_x}s+\frac{\pi^2(i-0.5)^2}{L^2I_xC_x}} & \sum_{i=1}^{m} \frac{\frac{(-1)^i(1-2i)\pi}{L^2I_xC_x}}{s^2+\frac{R_x}{I_x}s+\frac{\pi^2(i-0.5)^2}{L^2I_xC_x}} \end{bmatrix} \begin{bmatrix} P_{\text{in}}(s) \\ Q_{\text{out}}(s) \end{bmatrix}. \quad (36)$$

Note that at steady-state conditions, the analytical solution for transient pressure and flow oscillations of (11) becomes:

$$\begin{bmatrix} P_{\text{out}}(0) \\ Q_{\text{in}}(0) \end{bmatrix} = \begin{bmatrix} 1 & -LR_x \\ 0 & 1 \end{bmatrix} \begin{bmatrix} P_{\text{in}}(0) \\ Q_{\text{out}}(0) \end{bmatrix}. \quad (37)$$

However, these features are not presented in (36) due to the finite number of modes used to approximate transcendent transfer functions with an infinite number of modes. To correct the DC gains of the transfer functions in (36), two factors, C_1 and C_2, are included in the diagonal and upper off-diagonal transfer functions. The resulting model, the *distributed lumped parameter model*, is obtained as follows:

$$\begin{bmatrix} P_{\text{out}}(s) \\ Q_{\text{in}}(s) \end{bmatrix} = \begin{bmatrix} C_1\sum_{i=1}^{m} \frac{\frac{(-1)^i(1-2i)\pi}{L^2I_xC_x}}{s^2+\frac{R_x}{I_x}s+\frac{\pi^2(i-0.5)^2}{L^2I_xC_x}} & -C_2\sum_{i=1}^{m} \frac{\frac{2}{LC_x}s+\frac{R_x}{LI_xC_x}}{s^2+\frac{R_x}{I_x}s+\frac{\pi^2(i-0.5)^2}{L^2I_xC_x}} \\ \sum_{i=1}^{m} \frac{\frac{2}{LI_x}s}{s^2+\frac{R_x}{I_x}s+\frac{\pi^2(i-0.5)^2}{L^2I_xC_x}} & C_1\sum_{i=1}^{m} \frac{\frac{(-1)^i(1-2i)\pi}{L^2I_xC_x}}{s^2+\frac{R_x}{I_x}s+\frac{\pi^2(i-0.5)^2}{L^2I_xC_x}} \end{bmatrix} \begin{bmatrix} P_{\text{in}}(s) \\ Q_{\text{out}}(s) \end{bmatrix}, \quad (38)$$

where

$$C_1 = \left[\sum_{i=1}^{m} \frac{2(-1)^{i+1}}{\pi(i-0.5)}\right]^{-1}, \quad (39)$$

And

$$C_2 = \left[\sum_{i=1}^{m} \frac{1}{\pi^2(i-0.5)^2}\right]^{-1}. \quad (40)$$

Evaluation of the proposed approximations is performed using a comparison of the frequency response functions for the transcendent (exact) transfer functions,

$\cosh^{-1}(nL)$, $Z_K\tanh(nL)$ and $Z_K^{-1}\tanh(nL)$, and their rational approximations in (38) for the first eight modes. Provided in Table 1 are the fluid and line specifics used for the frequency responses in Figure 2. The proposed approximated model provides an accurate result by accurately predicting the corresponding resonant frequencies of (11).

$$\begin{bmatrix} P_{\text{out}} \\ Q_{\text{in}} \end{bmatrix} = \begin{bmatrix} C_1 \sum_{i=1}^{m} \frac{\kappa_i \frac{(-1)^i(1-2i)\pi}{L^2 I_x C_x}}{s^2+\tau_i \frac{R_x}{I_x} s+\kappa_i \frac{\pi^2(i-0.5)^2}{L^2 I_x C_x}} & -C_2 \sum_{i=1}^{m} \frac{\frac{2}{LC_x} s+\tau_i \frac{R_x}{LI_x C_x}}{s^2+\tau_i \frac{R_x}{I_x} s+\kappa_i \frac{\pi^2(i-0.5)^2}{L^2 I_x C_x}} \\ \sum_{i=1}^{m} \frac{\kappa_i \frac{2}{LI_x} s}{s^2+\tau_i \frac{R_x}{I_x} s+\kappa_i \frac{\pi^2(i-0.5)^2}{L^2 I_x C_x}} & C_1 \sum_{i=1}^{m} \frac{\kappa_i \frac{(-1)^i(1-2i)\pi}{L^2 I_x C_x}}{s^2+\tau_i \frac{R_x}{I_x} s+\kappa_i \frac{\pi^2(i-0.5)^2}{L^2 I_x C_x}} \end{bmatrix} \begin{bmatrix} P_{\text{in}} \\ Q_{\text{out}} \end{bmatrix}, \tag{41}$$

3.2. Modified distributed lumped parameter model

The *distributed lumped parameter model*, derived in the previous section, is obtained by solving (1)–(4) with the assumption that only the quasi-steady friction term contributes to losses (see Appendix 1), thereby neglecting unsteady friction and heat transfer effects. In this section, the obtained model in (38) is revised to include these second-order effects. The resulting model is the so-called *modified distributed lumped parameter model*. A similar approach to that presented by Yang and Tobler (1991) is used by adding two frequency-dependent modification factors τ_i and κ_i to correct the natural frequencies and damping ratio parameters of the model.

By comparing the momentum Equations (1) and (9), the resistance and inertance per unit length need to be adjusted to include unsteady friction effects. The resulting model can be written as:

where the expression of the factor, C_2, becomes:

$$C_2 = \left[\sum_{i=1}^{m} \frac{\tau_i}{\kappa_i \pi^2 (i-0.5)^2}\right]^{-1}. \tag{42}$$

Because the damping ratio in (41) has a new expression, the condition for underdamped lines in (16) is modified as:

$$\frac{\tau_1}{\sqrt{\kappa_1}} \frac{L}{\pi} R_x \sqrt{\frac{C_x}{I_x}} < 1. \tag{43}$$

To obtain τ_i and κ_i, the true natural frequencies and damping ratios of the *dissipative model* of (5) are first calculated numerically using the technique described by King (2006) for the case of liquid and air. These parameters are functions of the dimensionless characteristic root λ_{c_i} defined as:

Table 1. Case study parameters.

Flow	Laminar
Hydraulic line	Horizontal rigid pipe
Line length	1000 [m]
Line internal diameter	0.03 [m]
Line roughness	$1.5{\cdot}10^{-5}$ [m]
Liquid density	999 [kg/m^3]
Liquid dynamic viscosity	0.0015 [kg/m/s]
Speed of sound	1000 [m/s]

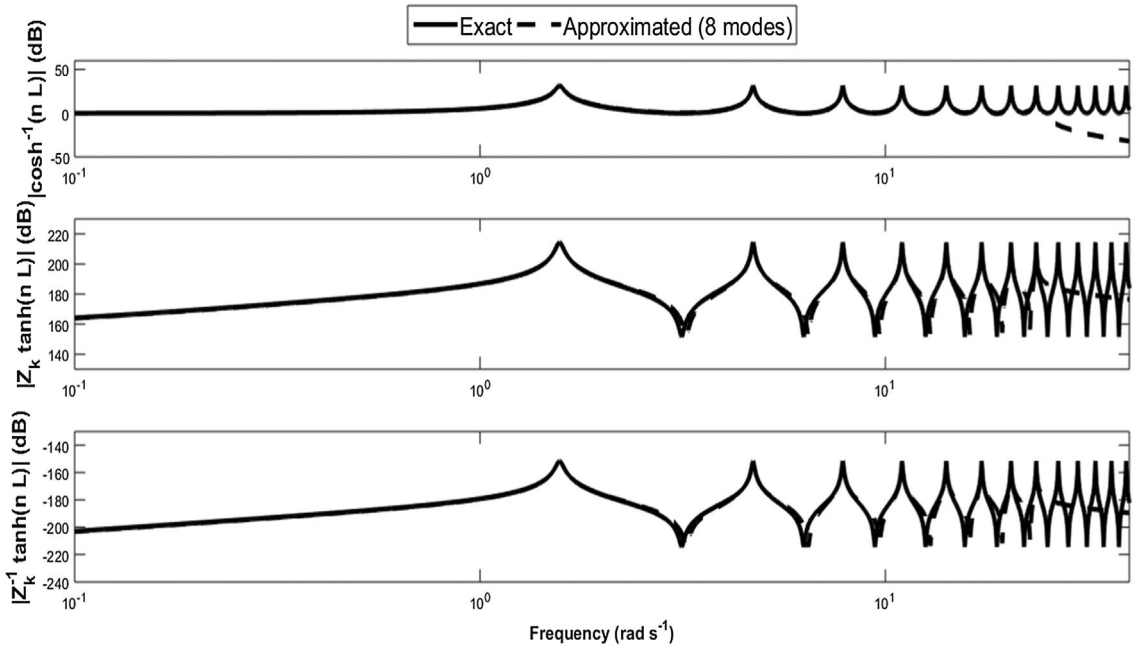

Figure 2. Frequency response comparison of the transcendent and the rational transfer functions.

$$\lambda_{c_i} = \frac{i - 0.5}{D_n}, \tag{44}$$

where D_n is the dissipation number (Yang and Tobler 1991):

$$D_n = \frac{LR_x}{8}\sqrt{\frac{C_x}{I_x}}. \tag{45}$$

The values of τ_i and κ_i are computed for the case of laminar flow in horizontal transmission lines by comparing the natural frequencies and damping ratios of (41) with those derived numerically from the modal approximation of the *dissipative model* (King 2006). Using logarithmic and hyperbolic functions, empirically determined functions are proposed to express the resulting frequency-dependent modification factors as functions of λ_{c_i}. The resulting τ_i and κ_i are given as:

$$\begin{aligned}\tau_i = {} & A_1 \tanh\left(A_2 \log_{10}\left(\lambda_{c_i}\right) + A_3\right) \\ & + A_4 \tanh\left(A_5 \log_{10}\left(\lambda_{c_i}\right) + A_6\right) + A_7,\end{aligned} \tag{46}$$

$$\begin{aligned}\log_{10}(\kappa_i) = {} & B_1 \tanh\left(B_2 \log_{10}\left(\lambda_{c_i}\right) + B_3\right) \\ & + B_4 \tanh\left(B_5 \log_{10}\left(\lambda_{c_i}\right) + B_6\right) + B_7,\end{aligned} \tag{47}$$

where the parameters A_i and B_i for both liquid and air cases are numerically obtained using MATLAB® Curve-Fitting Toolbox and they are given in Appendix 2. Illustrated in Figure 3 is a comparison between the numerically computed and analytically estimated values of the two modification factors.

To demonstrate the differences between the *distributed lumped parameter model*, the *modified distributed lumped parameter model* and the *dissipative model*, the frequency response functions for eight modes are compared. Illustrated in Figure 4 is the comparison result using the parameters presented in Table 1. As can be seen, the *modified distributed lumped parameter model* matches the *dissipative*, while the *distributed lumped parameter model* does not accurately predict transmission line dynamic characteristics because it neglects the unsteady friction losses. Similar agreement is observed for other fluid and line properties.

3.3. Accuracy of the modified distributed lumped parameter model for turbulent flow

Modelling turbulent flow in transmission lines is more complicated due to the turbulent frequency-dependent friction function. Numerical methods have been proposed to solve the problem of modelling unsteady turbulent flow in transmission lines. The most common method is based on weighting functions having certain approximations and assumptions. Johnston (2011a, 2011b) have developed numerical models for turbulent friction in both smooth-walled and rough pipes. The fluid velocity is calculated numerically for a range of viscosity distributions and frequencies to obtain the frequency-dependent friction. The computed results are in agreement with other numerical models proposed in the literature (Vitkovsky *et al.* 2004) for the case of smooth-walled pipes (Johnston 2011a). A test rig is also built to validate the turbulent unsteady friction models when including the effects of pipe roughness. Measured

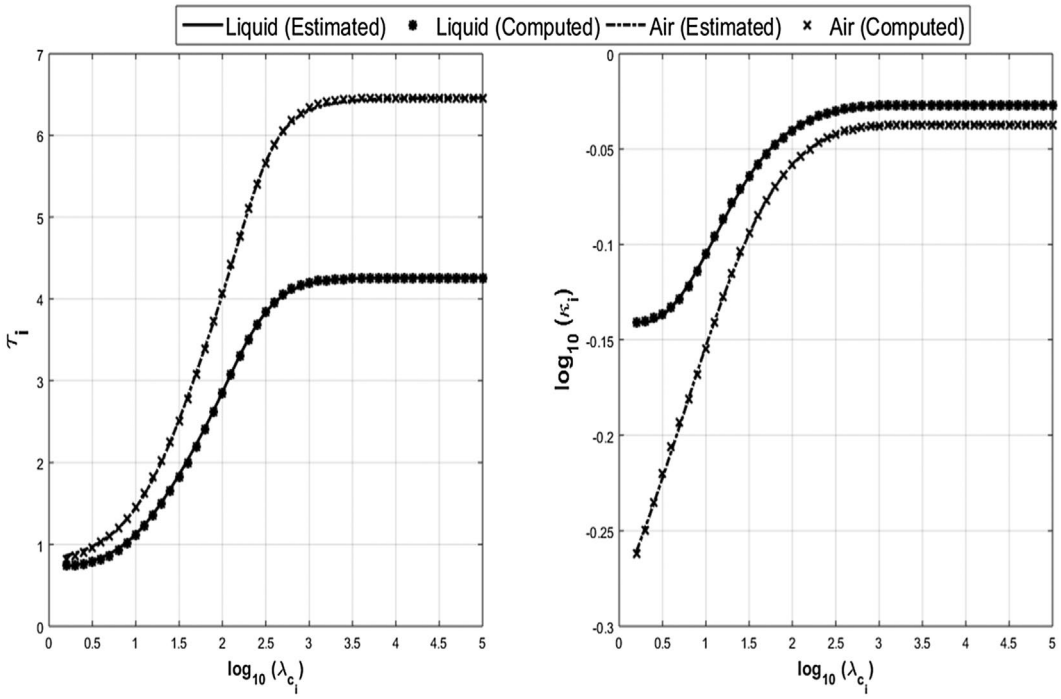

Figure 3. Frequency-dependent modification factors τ_i and κ_i.

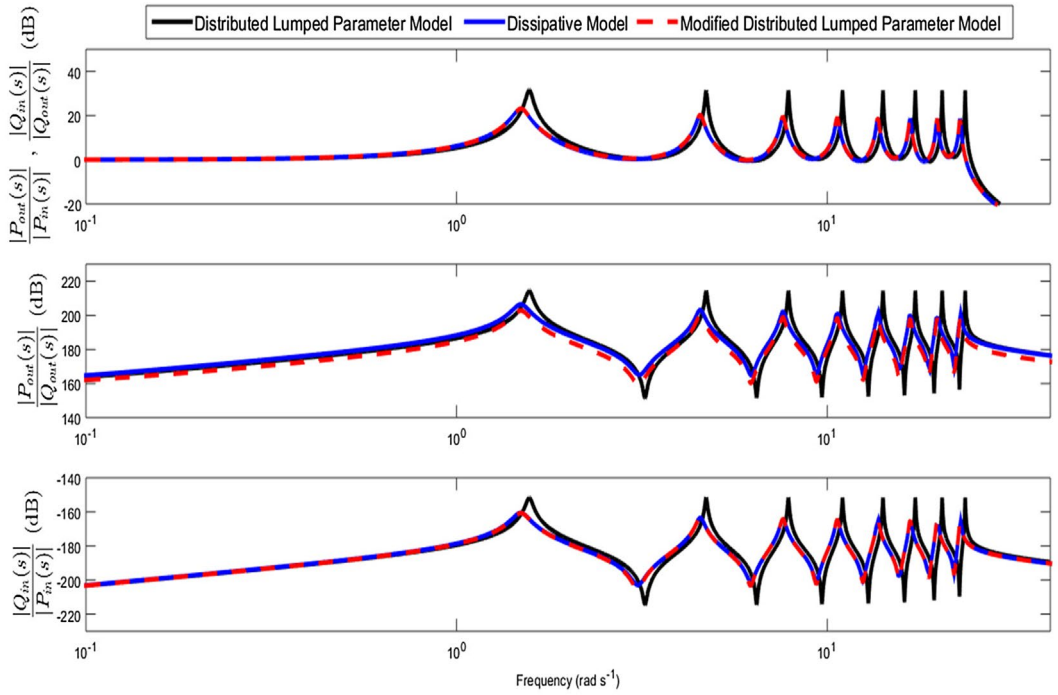

Figure 4. Frequency responses of the *Distributed Lumped Parameter Model*, the *Modified Distributed Lumped Parameter Model* and the *Dissipative Model*.

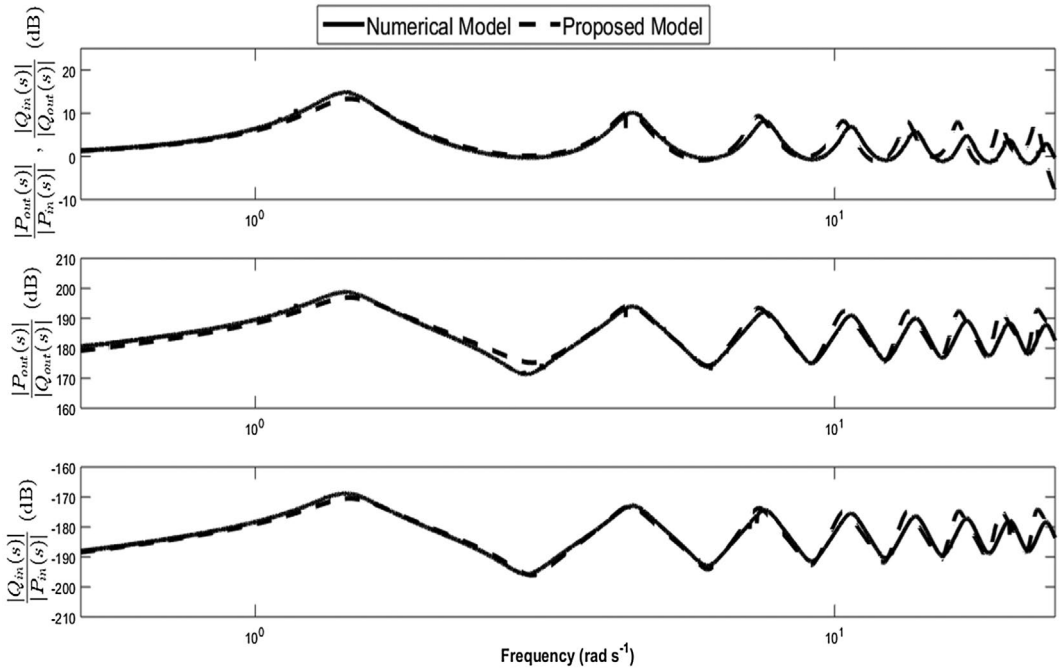

Figure 5. Comparison between the proposed model (41) and the numerical model (Johnston 2011a).

and simulated results show a good agreement (Johnston 2011b).

A comparison between the numerical model developed by Johnston (2011a) and the proposed model in (41) is conducted. The numerical model is simulated using the method of characteristics. The system is excited using pseudo-random binary sequence (PRBS) for the input signals for P_{in} and Q_{out}, over a broad frequency range. The amplitude of the excitation is chosen to be 10% about the steady-state values of the signals so that the system is simulated under small perturbations around the operating point. Both inputs (P_{in}, Q_{out}) and outputs (P_{out}, Q_{in}) are captured and then compared by calculating the FRFs using the Fast Fourier Transform (FFT) algorithm in combination with the Hanning window function. To compare the models, the simulated results are provided in Figure 5 using the data given in Table 1 except for the flow conditions where the flow is

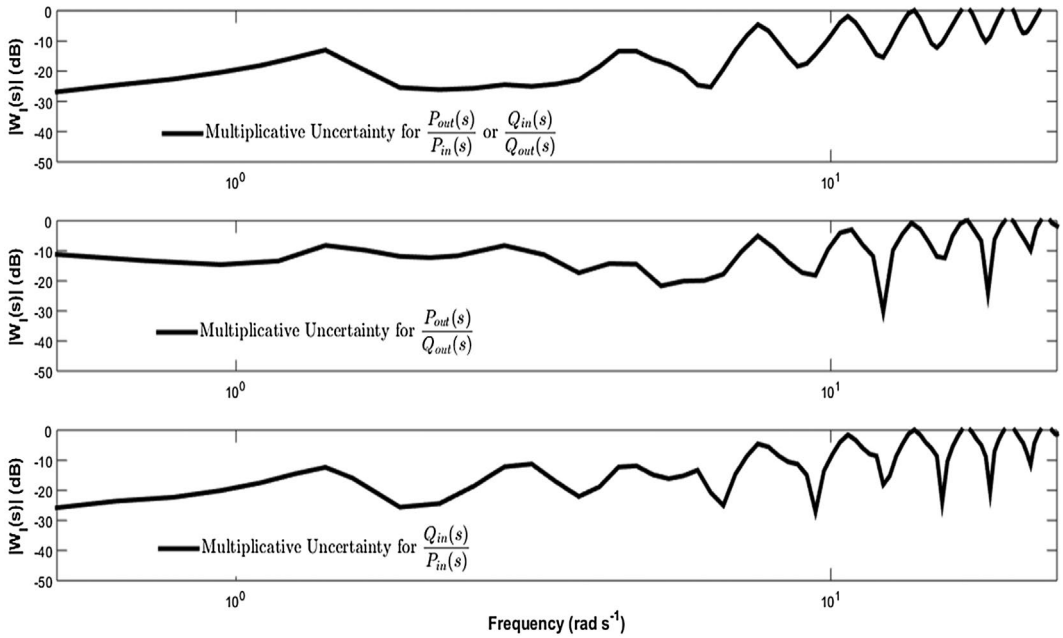

Figure 6. Corresponding multiplicative uncertainty.

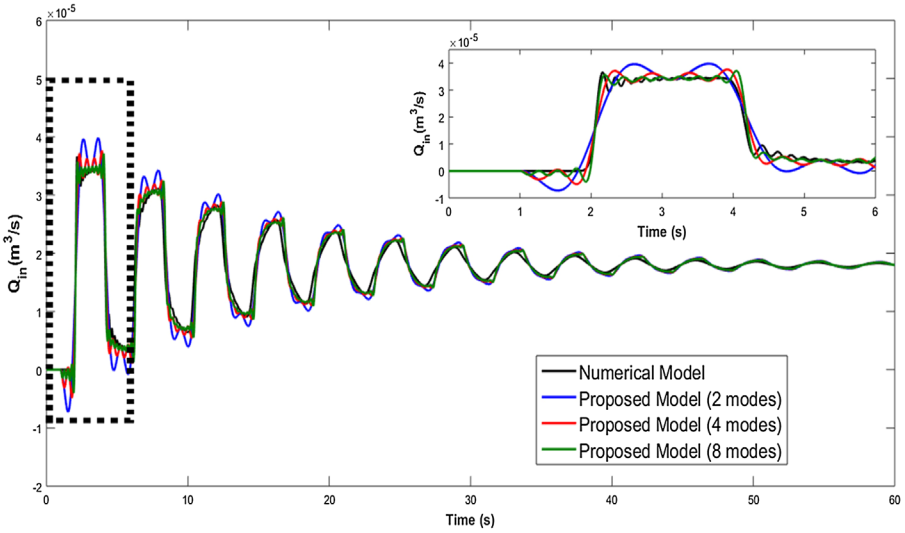

Figure 7. Step response comparison. Case 1: Laminar ($Re = 500$).

turbulent ($Re = 5000$). Figure 6 illustrates the discrepancies between the numerical model and the proposed model by calculating, over the frequency range of interest, the magnitude of the unstructured multiplicative uncertainty function $W_I(j\omega)$ defined as:

$$G(j\omega) = \tilde{G}(j\omega)\big(1 + W_I(j\omega)\Delta_I(j\omega)\big), \qquad (48)$$

where $G(j\omega)$ is the FRF from the numerical model in Johnston (2011a), $\tilde{G}(j\omega)$ is the FRF of the proposed model (41) and $\Delta_I(j\omega)$ is any stable transfer function upper bounded as $\left|\Delta_I(j\omega)\right| \leq 1, \forall\omega$. Agreement between the two models is observed despite the fact that the second-order effects are introduced in the two models differently. Johnston (2011a) has made several simplifications and assumptions to approximate the true frequency-dependent friction losses for the turbulent flow case. In the proposed model, the unsteady friction effects are included using results from the *dissipative model*, which is only valid for the case of laminar flow with only steady friction losses are adjusted. This results in small discrepancy between the two models. Similar observations are obtained for different flow conditions, fluid properties and transmission line geometry.

To further examine the accuracy of the proposed model, pressure and flow step responses of (41) with different number of modes are simulated and compared with those of the numerical model for different boundary conditions, fluid properties and transmission line geometry. Shown in Figures 7 and 8 are the flow rate step responses at the inlet of the transmission line for the cases of laminar and turbulent flow, respectively. Fluid

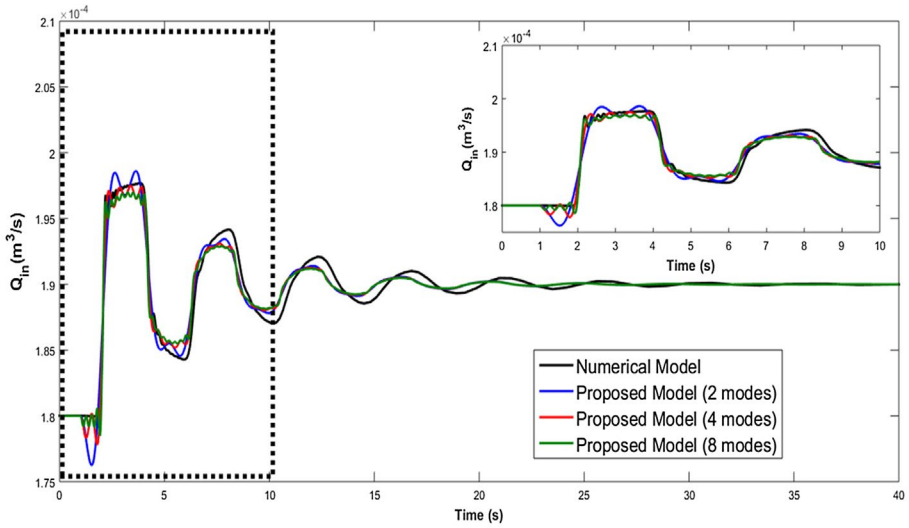

Figure 8. Step response comparison. Case 2: Turbulent ($Re = 5000$).

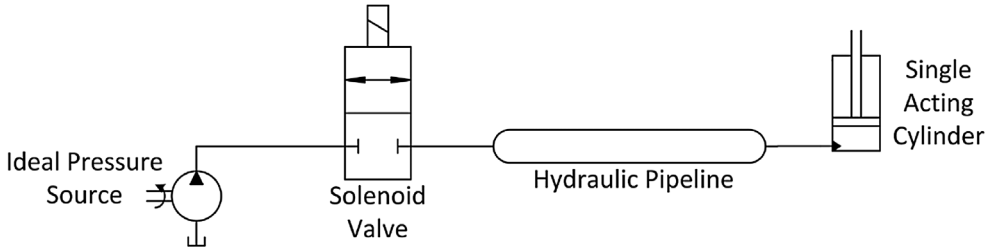

Figure 9. Schematic of the fluid power system.

characteristics and line geometry are given in Table 1. As can be seen in Figure 7, the proposed model matches the numerical model for the laminar flow case, particularly when the number of modes included in the approximation is sufficiently high. A performance metric is used to evaluate the accuracy of the proposed model by comparing its response to that of the numerical model in the time domain. This measure, the *weighted mean absolute percentage error* (*WMPAE*) defined in (49), is appropriate for data that have some values that are equal or close to zero (Kolassa and Schutz 2007).

$$WMPAE = 100 \sum_{i=1}^{n} \frac{|y_i - \hat{y}_i|}{\sum_{k=1}^{n} y_k} \tag{49}$$

The *WMPAE* between the step response given by the numerical model and that obtained by the proposed eight-mode model is equal to 4%, whereas it is equal to 9% and 7% for the case of two-mode and four-mode models, respectively. Thus, transient response estimations including time delay are improved with the number of modes increasing.

For the turbulent flow case, increasing the number of modes also improves the time delay representation but does not improve the transient response estimation of the proposed model response compared with that of the numerical model (Figure 8). The *WMAPE* between the step response of the numerical model and that given by the three models, namely the two-mode, four-mode and eight-mode models, is less than 1%. The discrepancy between the numerical model and the proposed model in the over- and under-shoots is due to the difference in assumptions and simplifications made to characterise turbulent unsteady friction effects. However, despite the significant differences between the two approaches, the simulation results show acceptable agreement between the two models. As will be illustrated in the following section, one major advantage the proposed model has over the numerical model is that it is written in rational transfer function form and its coefficients are explicitly obtained given the fluid properties and transmission line geometry. This simplifies simulation analysis, especially when the transmission line is one component of a total complex system composed of other components, such as pumps, valves and actuators.

4. Fluid power system design example

Presented in this section is a fluid power design example illustrating the utility of the proposed model in (41). The system is composed of an ideal pressure source, a directional (solenoid) valve, a hydraulic single-acting cylinder and a smooth hydraulic line connecting the two latter components (Figure 9), which are modelled as hydraulic two-port networks (Manhartsgruber 2009). The goal of the system design is to select the line sizing

to avoid vibrations of the system components due to pressure and flow oscillations when operating the cylinder (i.e. opening the valve). This translates into finding optimal lengths and diameters of the transmission line such that transient pressure peaks do not exceed half of the supply pressure and the cylinder closing time is less than five seconds.

A mathematical physics-based model of each component is developed with the assumptions that the cylinder has no loading on its piston and no leakage (internal or external) is taken into account for all components. The system parameters, design parameters and operating condition are summarised in Table 2. The resulting models for the valve and the cylinder can be expressed as

$$\text{Directional valve:} \quad Q_0 = \frac{1}{\tau_v s + 1} C_d A_v \sqrt{\frac{2}{\bar{\rho}}} \sqrt{P_s - P_0}. \tag{50}$$

$$\text{Single-acting cylinder:} \quad Q_L = \frac{A_c^2 P_L s}{c_c s + k_c}. \tag{51}$$

To achieve the design goal, a model of the total system is first built in MATLAB® Simulink using Equations (41), (50) and (51). A script is then created to automatically simulate the performance of the system for any possible configuration within the defined design space and save model outputs (i.e. pressures, flow rates and cylinder displacement). The designs that meet the defined performance requirements (successful designs) are finally selected. The results are presented in Figure 10.

Because it is defined in analytical form and can be simulated in time domain, the model in (41) can be integrated with other analytical time domain models. This introduces modelling and simulation flexibility of fluid power systems while still maintaining accuracy and complexities. The use of simpler but less accurate analytical model of transmission lines may results into inappropriate solutions. In fact, the proposed model is replaced with the conventional lumped parameter model of (8). As can be seen in Figure 10, the resulting successful designs using this model are different for those obtained using the proposed model.

5. Conclusion

Models for laminar and turbulent flow in transmission lines using distributed lumped parameters were derived. Three transcendent transfer functions were obtained by solving the Navier-Stokes equations and assuming that only quasi-steady friction effects contribute to losses. These transfer functions are then approximated by finite-order rational polynomial transfer functions for the case of underdamped lines using residue theorem.

Table 2. Design example parameters.

Fluid	Density $\bar{\rho}$ [kg/m^3]	999
	Absolute viscosity μ [kg/m/s]	1.5E-3
	Bulk modulus β_e [Pa]	1.5E9
Source	Pressure P_s [Pa]	2E7
Solenoid valve	Discharge coefficient C_d	0.7
	Spool dynamics time constant τ_v [s]	0.1
	Maximum orifice area A_v [m^2]	8E-6
Single-acting cylinder	Piston Area A_c [m^2]	4E-3
	Spring stiffness k_c [kg/s^2]	9E5
	Cylinder viscous damping c_c [kg/s]	9E5
Design parameters	Minimum, Maximum line diameter [m]	7E-3, 12E-3
	Minimum, Maximum line length [m]	0.5, 3

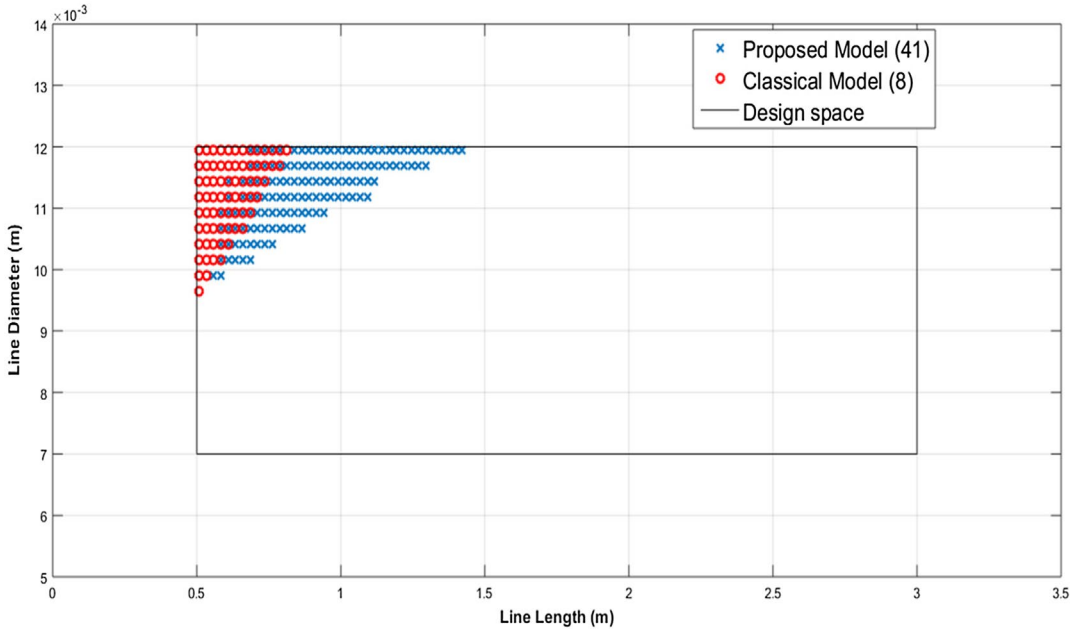

Figure 10. Successful design using the *Modified Distributed Lumped Parameter Model* (41) and the classical lumped parameter model (8).

Due to the finite number of modes being used in the approximation, a low frequency gain correction was applied. Unlike the *dissipative model*, the *distributed lumped parameter model* do not account for the unsteady friction and heat transfer effects. Therefore, frequency-dependent effects are extracted from the *dissipative model* and the results are incorporated in the *distributed lumped parameter model* by adding two modification factors. The resulting model called the *modified distributed lumped parameter model* can be applied for both laminar and turbulent flow cases. In the case of turbulent flow, the overall model depends on the operating conditions (i.e. flow rate), and therefore, it is approximated by a combination of locally linear models derived for a constant average Reynolds number. A major advantage of the proposed model over existing models is that its coefficients are expressed analytically as functions of the transmission line and fluid parameters rather than tables or graphs. The accuracy of the proposed model was investigated by comparing its frequency responses with those of the *dissipative model* in the case of laminar flow. In the turbulent flow case, the proposed model is compared with a reliable numerical model showing acceptable coincidence. To demonstrate the effectiveness of the proposed model, a design problem of a fluid power system comprised of a transmission line, a valve and an actuator is finally formulated and presented.

Acknowledgements

The authors gratefully acknowledge the valuable input of the engineering team in the Technology and Innovation Department at Transocean.

Disclosure statement

No potential conflict of interest was reported by the authors.

Notes on contributors

Taoufik Wassar is a research assistant professor at University of Houston in the Mechanical Engineering Department. He received his PhD in Mechanical Engineering from University of Houston in 2014 and his BSc in Mechanical Engineering from Tunisia Polytechnic School in 2008. His expertise is in model-based methods for diagnostics and control of automotive, biomedical and energy systems. In his doctoral and postdoctoral research, Wassar has worked with the Texas Heart Institute to model, control and diagnose in real-time total artificial heart. In collaboration with the physicians at THI, he completed animal studies to validate his work. He has also worked with Ford to detect and electronically trim cylinder-to-cylinder air/fuel ratio imbalance in a direct injection engine.

Matthew A Franchek is the founding director of the University of Houston Subsea Engineering Program. He received his PhD in Mechanical Engineering from Texas A&M University in 1991 and started his career at Purdue University as an assistant professor in Mechanical Engineering. He was promoted to an associate professor with tenure in 1997 and then to full professor in 2001. While at Purdue, he initiated and led two industry supported interdisciplinary research programs: an Automotive Research Program and an Electro-Hydraulic Research Program. From 2002 to 2009, he served as Chair of Mechanical Engineering at UH while simultaneously initiating the UH Biomedical Engineering undergraduate program. After his term as Department Chair, Franchek worked with Houston area companies to create the nation's first subsea engineering program. His expertise is in model-based methods for diagnostics and control of aerospace, automotive, biomedical and energy systems. His current research program focuses on multiphase pipeline flow, artificial lift, blowout preventers and electrical power distribution. He has authored over 70 archival publications, and over 100 conference publications. He has served as the advisor to 18 doctoral students and 31 masters students.

José A Gutierrez is the director of technology and innovation at Transocean focused on the delivery of sustainable innovation tailored for the Oil and Gas industry. His efforts are framed in the execution of business and technology development activities that enable the introduction of new products designed to augment operational integrity in Deepwater offshore drilling operations. In addition, Gutierrez is Adjunct Professor of Subsea Engineering in the Cullen School of Engineering at the University of Houston providing guidance on relevant research topics aligned to the business needs of the industry. Gutierrez has more than 20 years of experience managing innovation and technology strategy for companies such as Emerson Electric and Eaton Corporation.

References

Brown, F.T., 1962. The transient response of fluid lines. *Journal of Basic Engineering, ASME Transactions*, 84 (4), 547–553.

Blažič, S., Matko, D. and Geiger, G., 2004. Simple model of a multi-batch driven transmission line. *Mathematics and Computers in Simulation*, 64, 617–630.

Colebrook, C.F., 1939. Turbulent flow in pipes, with particular reference to the transition region between smooth and rough pipe laws. *Journal of the Institution of Civil Engineers*, 11, 133–156.

D'Souza, A.F. and Oldenburger, R., 1964. Dynamic Response of Fluid Lines. *Journal of Fluids Engineering, ASME Transactions*, 86 (3), 589–598.

Doebelin, E.O. and Swisher, G.M., 1970. Lumped-parameter modeling vs distributed- parameter modeling for fluid control lines. *Journal of Spacecraft and Rockets*, 7 (6), 766–767.

Gerlach, C.R., 1969. Dynamic models for viscous fluid transmission lines. *Proceedings of the 10th Joint Automatic Control Conference*, Boulder, Colorado.

Goodson, R.E. and Leonard, R.G., 1972. A survey of modeling techniques for fluid line transients. *Journal of Basic Engineering, Transaction of ASME*, 94, 474–482.

Goudar, C.T. and Sonnad, J.R., 2008. Comparison of the iterative approximations of the Colebrook-White equation. *Hidrocarbon Processing*, 87 (8), 79–83.

Hsue, C.Y., and Hullender, D.A., 1983. Modal approximations for the fluid dynamics of hydraulic and pneumatic transmission lines. *Fluid Transmission Lines Dynamics*. ASME Special Publication, 2, New York.

Howie, J.M., 2004. *Complex analysis*. London: Springer-Verlag.

Iberall, A.S., 1950. Attenuation of oscillatory pressures in instrument lines. *Journal of Research of the National Bureau of Standards*, 45 (1), 85.

Johnston, D.N., 2011. Numerical modelling of unsteady turbulent flow in smooth-walled pipes. *Proceedings of the Institution of Mechanical Engineers, Part C: Journal of Mechanical Engineering Science*, 225 (7), 1601–1615.

Johnston, D.N., 2011. Numerical modelling of unsteady turbulent flow in tubes, including the effects of roughness and large changes in Reynolds number. *Proceedings of the Institution of Mechanical Engineers, Part C: Journal of Mechanical Engineering Science*, 225 (8), 1874–1885.

Johnston, D.N., 2012. The transmission line method for modeling laminar flow of liquid in transmission lines. *Proceedings of the Institution of Mechanical Engineers, Part I: Journal of Systems and Control Engineering*, 226 (5), 586–597.

King, J.D., 2006. *Frequency response approximation methods of the dissipative model of fluid transmission lines*. Thesis (Master of Science Degree in Mechanical Engineering). University of Texas, Arlington, Texas.

Kogler, H., Manhartsgruber, B. and Haas, R., 2007. A Fourier-Galerkin-Newton method for periodic nonlinear transmission line problems. *Power Transmission and Motion Control*, 217–227.

Kolassa, S., Schutz, W., 2007. Advantages of the MAD/mean ratio over the MAPE. *Foresight: the International Journal of Applied Forecasting*, 6, 40–43.

Mamis, M.S. and Koksal, M., 2000. Remark on the lumped parameter modeling of transmission lines. *Electric Machines & Power Systems*, 28 (6), 565–575.

Manhartsgruber, B., 2005. Reduced order, discrete-time, input-output modelling of laminar pipe flow. *IASME Transactions*, 2 (6), 911–918.

Manhartsgruber, B., 2006. On the passivity of a Galerkin Finite element model for transient flow in hydraulic pipelines. *Proceedings of the Institution of Mechanical Engineers, Part I: Journal of Systems and Control Eng.*, 220 (3), 223–237.

Manhartsgruber, B., 2009. Identification of the input-output behaviour of hydraulic two-port networks. *Proc. ASME Dynamic Systems and Control Conference*, October 2009, Hollywood, CA.

Matko, D., Geiger, G. and Gregoritza, W., 2000. Transmission line simulation techniques. *Mathematics and Computers in Simulation*, 52, 211–230.

Matko, D., Geiger, G. and Werener, T., 2001. Modelling of the transmission line as a lumped parameter system. *AUTOMATIKA*, 42 (3–4), 177–188.

Meziou, A., Chaari, M., Franchek, M., Borji, R., Grigoriadis, K. and Tafreshi, R., 2016. Low-dimensional modeling of transient two-phase flow in pipelines. *Journal of Dynamic Systems, Measurement, and Control*, 138 (10), 101008.

Mikota, G., 2013. Modal analysis of hydraulic pipelines. *Journal of Sound and Vibration*, 332 (16), 3794–3805.

Oldenburger, R. and Goodson, R.E., 1964. Simplification of hydraulic line dynamics by use of infinite products. *Journal of Basic Engineering, AMSE Transactions*, 86, 1–8.

Rachford, H.H., and Ramsey, E.L., 1975. Application of variational methods to model transient flow in complex liquid transmission systems. *Society of Petroleum Engineers of AIME*, 50th Annual Fall Meeting, Dallas, Texas.

Rao, C.V. and Eswaran, K., 1993. On the analysis of pressure transients in transmission lines carrying compressible fluids. *International Journal of Pressure Vessels And Piping*, 56, 107–129.

Rufelt, A., 2010. Numerical studies of unsteady. Friction in transient pipe flow. Master of Science Thesis. Stockholm, Sweden.

Soumelidis, M.I., Johnston, D.N., Edge, K.A. and Tilley, D.G., 2005. *A comparative study of modelling techniques for laminar flow transients in hydraulic transmission lines*. Tsukuba: Sixth JFPS International Symposium on Fluid Power.

Stecki, J.S. and Davis, D.C., 1986. Fluid transmission lines distributed parameter models part 1: a review of the state of the art. *Proceedings of the Institution of Mechanical Engineers, Part A: Power & Process Engineering*, 200 (4), 215–228.

Streeler, V.L. and Lai, C., 1962. Water-hammer analysis including fluid friction. *Journal of the Hydraulics Division*, 88, 79–112.

Vitkovsky, J., Stephens, M., Bergant, A., Lambert, M. and Simpson, A., 2004. Efficient and accurate calculation of Ziekle and Vardy-Brown unsteady friction in pipe transients. *9th International Conference on Pressure Surges*, Chester, United Kingdom, 24–26.

Woods, R.L., 1981. *The effects of source and load impedance connected to fluid transmission lines*. New York: Fluid Transmission Lines Dynamics, ASME Special Publication.

Yang, W.C., 1983. Modal approximation of hydraulic transmission line models by using simplified bessel function ratio. Thesis (Master of Science Degree in Mechanical Engineering). University of Texas, Arlington, Texas.

Yang, W.C. and Tobler, W.E., 1991. Dissipative Modal Approximation of Fluid Transmission Line Using Linear Friction Model. *Journal of Dynamic Systems, Measurement, and Control, Transactions of the ASME*, 113, 152–162.

Appendix 1

The unsteady flow problem in a cylindrical transmission line can be described using the set of partial differential Equations (1)–(4). By neglecting heat transfer losses and adding the effects of gravity, this system of equations can be written in a one-dimensional-form as (Rufelt 2010):

$$\frac{\bar{\rho}}{A}\frac{\partial Q}{\partial t}+\frac{\partial P}{\partial x}+\bar{\rho}g\sin\theta+f(Q)=0, \tag{A.1}$$

$$\frac{\partial P}{\partial t}+\frac{c^2\bar{\rho}}{A}\frac{\partial Q}{\partial x}=0, \tag{A.2}$$

where Q [m^3/s] is the fluid flow rate, A is the line cross-sectional area [m^2], $\bar{c}$ is the average speed of sound in the fluid, g is the gravity constant [m/s^2], θ is the angle of the line inclined with respect to the horizontal [rad], and $f(Q)$ is the friction term, defined as:

$$f(Q)=f_s(Q)+f_u(Q), \tag{A.3}$$

with $f_s(Q)$is the contribution of quasi-steady flow line resistance and $f_u(Q)$is the contribution of the frequency-dependent flow line resistance (Rufelt 2010). The quasi-steady friction term can be computed using Darcy and Weisbach formula (Colebrook 1939):

$$f_s(Q)=\frac{\lambda_Q}{2D_iA^2}\bar{\rho}Q|Q|, \tag{A.4}$$

where D_i [m] is the inner diameter of the line and λ_Q is the dimensionless Darcy–Weisbach friction factor. For the case of laminar flow ($Re \le 2300$), the friction factor is (Colebrook 1939):

$$\lambda_Q=\frac{64}{Re}=\frac{64\mu A}{\bar{\rho}D_i|Q|}. \tag{A.5}$$

For transitional and turbulent flow ($Re > 2300$), λ_Q can be calculated using the Goudar–Sonnad explicit equation (Goudar and Sonnad 2008):

$$\frac{1}{\sqrt{\lambda_Q}}=0.8686\ln\left(\frac{0.4587\,Re}{(M-0.31)^{\frac{M}{M+1}}}\right), \tag{A.6}$$

where

$$M=0.124\,Re\frac{\varepsilon}{D_i}+\ln(0.4587\,Re) \tag{A.7}$$

and ε is the line roughness [m].

As discussed by Rufelt (2010), the unsteady friction term, $f_u(Q)$, represents the additional friction losses due to viscous losses caused by the two-dimensional (three-dimensional) behaviour of the velocity profile for the case of laminar flow (turbulent flow). To retain a one-dimension model, the effects of the unsteady friction are temporarily neglected ($f_u(Q)=0$).

Substituting (A.4) into (A.3) and then into (A.1) gives:

$$\frac{\bar{\rho}}{A}\frac{\partial Q}{\partial t}+\frac{\partial P}{\partial x}+\bar{\rho}g\sin\theta+\frac{\lambda_Q}{2D_iA^2}\bar{\rho}Q|Q|=0. \tag{A.8}$$

The partial differential equations in (A.2) and (A.8) can now be written as (Matko *et al.* 2001):

$$I_x\frac{\partial Q}{\partial t}+R_xQ=-\frac{\partial P}{\partial x}, \tag{A.9}$$

$$C_x\frac{\partial P}{\partial t}=-\frac{\partial Q}{\partial x}, \tag{A.10}$$

where R_x, I_x and C_x are the resistance, inertance and capacitance per unit length, respectively, defined as:

$$R_x=\bar{\rho}g\sin\theta\frac{1}{\bar{Q}}+\frac{\lambda_{\bar{Q}}\bar{\rho}}{2D_iA^2}|\bar{Q}|, \tag{A.11}$$

$$I_x=\frac{\bar{\rho}}{A}, \tag{A.12}$$

$$C_x=\frac{A}{\bar{c}^2\bar{\rho}}, \tag{A.13}$$

with $\bar{Q}$ and $\lambda_{\bar{Q}}$ are the nominal flow rate and nominal friction factor, respectively.

Appendix 2

Table B1. Values of the parameters A_k and B_k.

	Liquid	Air
A_1	0.920	2.050
A_2	1.500	1.300
A_3	−2.100	−2.100
A_4	0.870	0.800
A_5	2.000	2.530
A_6	−4.320	−5.780
A_7	2.470	3.610
B_1	0.100	0.275
B_2	1.143	0.665
B_3	−1.147	−0.649
B_4	−0.127	−0.100
B_5	0.716	0.702
B_6	0.455	−1.323
B_7	0.000	−0.213